

Published in final edited form as:

*Endocrinology*. 2007 August ; 148(8): 4091–4101. doi:10.1210/en.2007-0240.

## Estrogen Signaling via a Linear Pathway Involving Insulin-Like Growth Factor I Receptor, Matrix Metalloproteinases, and Epidermal Growth Factor Receptor to Activate Mitogen-Activated Protein Kinase in MCF-7 Breast Cancer Cells

Robert X.-D. Song, Zhenguo Zhang, Yucai Chen, Yongde Bao, and Richard J. Santen

Department of Internal Medicine (R.X.-D.S., Z.Z., Y.C., R.J.S.) and Biomolecular Research Facility (Y.B.), University of Virginia School of Medicine, Charlottesville, Virginia 22903

### Abstract

We present an integrated model of an extranuclear, estrogen receptor- $\alpha$  (ER $\alpha$ )-mediated, rapid MAPK activation pathway in breast cancer cells. In noncancer cells, IGF-I initiates a linear process involving activation of the IGF-I receptor (IGF-IR) and matrix metalloproteinases (MMP), release of heparin-binding epidermal growth factor (HB-EGF), and activation of EGF receptor (EGFR)-dependent MAPK. 17 $\beta$ -Estradiol (E2) rapidly activates IGF-IR in breast cancer cells. We hypothesize that E2 induces a similar linear pathway involving IGF-IR, MMP, HB-EGF, EGFR, and MAPK. Using MCF-7 breast cancer cells, we for the first time demonstrated that a sequential activation of IGF-IR, MMP, and EGFR existed in E2 and IGF-I actions, which was supported by evidence that the selective inhibitors of IGF-IR and MMP or knockdown of IGF-IR all inhibited E2- or IGF-I-induced EGFR phosphorylation. Using the inhibitors and small inhibitoryRNA strategies, we also demonstrated that the same sequential activation of the receptors occurred in E2-, IGF-I-, but not EGF-induced MAPK phosphorylation. Additionally, a HB-EGF neutralizing antibody significantly blocked E2-induced MAPK activation, further supporting our hypothesis. The biological effects of sequential activation of IGF-IR and EGFR on E2 stimulation of cell proliferation were also investigated. Knockdown or blockade of IGF-IR significantly inhibited E2- or IGF-I-stimulated but not EGF-induced cell growth. Knockdown or blockade of EGFR abrogated cell growth induced by E2, IGF-I, and EGF, indicating that EGFR is a downstream molecule of IGF-IR in E2 and IGF-I action. Together, our data support the novel view that E2 can activate a linear pathway involving the sequential activation of IGF-IR, MMP, HB-EGF, EGFR, and MAPK.

BREAST CANCER IS the most common neoplasm among women in Western countries and the second leading cause of cancer-related deaths in the United States. Two thirds of breast cancers are estrogen receptor  $\alpha$  (ER $\alpha$ ) positive. When activated by 17 $\beta$ -estradiol (E2), ER $\alpha$  plays an important role in the stimulation of cancer cell proliferation and prevention of apoptosis (1). The biological actions of E2 are mediated both by genomic transcriptional effects in the nucleus and by nongenomic actions via ER $\alpha$  acting outside of the nuclear compartment. Depending on the cell type and context, the nongenomic effects of E2 can lead to the rapid activation of many signaling molecules, such as 1) IGF-I receptor (IGF-IR) and epidermal growth factor receptor (EGFR), 2) p21<sup>ras</sup> and Raf-1, 3) MAPK and Akt, 4) protein kinase C,

Copyright © 2007 by The Endocrine Society

Address all correspondence and requests for reprints to: Richard J. Santen, Division of Endocrinology, University of Virginia Health Science Center, Charlottesville, Virginia 22903. E-mail: rjs5y@virginia.edu.

Disclosure Statement: The authors have nothing to disclose.

5) release of nitric oxide and stimulation of prolactin secretion, and 6) alteration of calcium and Maxi-K channels (2,3). Both genomic and nongenomic actions of E2 play pivotal roles in E2-induced cancer cell proliferation and survival (4).

Blockade of E2 synthesis with aromatase inhibitors or antagonism of its action with antiestrogens represents first-line treatments for patients with ER-positive breast cancer. However, primary or secondary resistance to hormonal therapy commonly occurs and may reflect enhanced activation of the growth factor receptor functions of IGF-IR and EGFR as well as human EGFR-2 (HER2/Neu) (5,6). Accumulating evidence suggests that ER $\alpha$  is involved in the development of hormone resistance, in which extranuclear actions of this receptor are operative (7). Our previously published work and that of others suggest a mechanistic link between growth factor pathways and extranuclear ER $\alpha$  in breast cancer cells whereby ER $\alpha$  binds to the IGF-IR and activates its downstream signaling pathways (8,9).

IGF-IR is important in cellular biological processes, including cell differentiation and proliferation, the establishment and maintenance of transformation, and protection against apoptosis (6). It is a hetero-tetrameric transmembrane glycoprotein comprising two  $\alpha$ - and two  $\beta$ -subunits. The  $\beta$ -subunits express intrinsic tyrosine kinase activity upon ligand binding to the  $\alpha$ -subunits. The EGFR is a type I receptor tyrosine kinase that mediates many biological processes, including cell migration, proliferation, and protection from apoptosis in response to ligands such as EGF and heparin-binding EGF (HB-EGF) (10). Interestingly, both IGF-IR and EGFR initiate some common downstream signaling pathways, such as activation of MAPK and Akt cascades (11). Ligand binding on the receptors initiates autophosphorylation of the receptor at tyrosine residues and activates IGF-IR or EGFR. A variety of docking proteins, such as the adapter protein Shc, insulin receptor substrate 1 (IRS-1), and the p85 $\alpha$ -subunit of phosphatidylinositol 3'-kinase (PI3K) that contain Src homology-2- and phosphotyrosine-binding domains, bind to the phosphorylated tyrosine residues on the receptors, leading to activation of the downstream signaling cascade of MAPK and Akt. Shc is a key regulatory element in the activation of the MAPK pathway, which is generally considered to provide growth-stimulating signals (12). Akt is a main substrate of PI3K and is known to play a major role in protection against cell apoptosis.

In recent studies, EGFR has been demonstrated to be a nodal point of convergence for many membrane cytokine receptors on MAPK activation (Fig. 1). For example, the receptors for GH, prolactin, integrin, and G protein-coupled receptors, such as the receptors for endothelin, lysophosphatidic acid, angiotensin, and thrombin, all require the EGFR as a central molecule on MAPK activation (13–15). Recently, IGF-I was identified to be another ligand using EGFR for MAPK activation (16,17). Using COS-7 cells, Roudabush *et al.* (18) demonstrated that this pathway requires the involvement of matrix metalloproteinases 2 and 9 (MMP2 and MMP9), cleavage of HB-EGF, and phosphorylation of the EGFR, leading to subsequent activation of MAPK. An integrating feature of this linear pathway is that the EGFR serves as a nodal point transducing signals initiated by many different ligands to MAPK.

E2 is known to rapidly activate many signaling molecules, including IGF-IR, EGFR, and MAPK in MCF-7 breast cancer cells (8,19,20). We previously demonstrated that in MCF-7 breast cancer cells, rapid ER $\alpha$  membrane translocation and its interaction with membrane IGF-IR are prerequisite steps for E2-induced MAPK activation (8). However, the integrated features among these molecules are poorly understood. Based on the linear pathway concept, we now raise the hypothesis that the IGF-IR activation induced by E2 can trigger a downstream signaling cascade through MMP2, MMP9, HB-EGF, and the EGFR and then activate MAPK (Fig. 1). The data presented in this manuscript provide strong evidence in support of this possibility. Our strategy to prove this hypothesis involved examination of the sequential molecular events occurring within minutes of adding E2 and the blockade or knockdown of

selective molecules by inhibitors, neutralizing antibodies, and small inhibitory RNAs (siRNAs). In addition, we used a reductionist approach that involved addition of the downstream mediators IGF-I and EGF in the absence of E2 to precisely determine the linear sequence of events. Taken together, our data demonstrated that a linear activation of IGF-IR, MMP, HB-EGF, and EGFR is required for E2 to activate MAPK. As a biological consequence, we demonstrated the role of this linear pathway on the stimulation of proliferation of breast cancer cells and protection against apoptosis.

## Materials and Methods

### Reagents

Tissue culture supplies were obtained from Fisher Scientific (Pittsburgh, PA). Improved MEM (IMEM) with or without phenol red (zinc option Richter's modification) and fetal bovine serum (FBS) were products of Gibco Life Technologies (Rockville, MD). E2 was obtained from Steraloids (Wilton, NH) and was dissolved in ethanol with a final concentration of ethanol in medium of less than 0.01%. IGF-I and EGF were purchased from R&D Systems (Minneapolis, MN). Both IGF-I and EGF were dissolved in PBS containing 10 mM acetic acid and 0.1% BSA as stock solution. The smartpool of double-stranded siRNA of IGF-IR (catalog no. M-003012-04), EGFR (M-003114-00-05) and siControl RNAs (D-001210-01-05) were from Dharmacon Tech (Lafayette, CO). All siRNAs were dissolved in RNase-free buffer based on the manufacturer's protocol at the concentration of 20  $\mu$ M. Tyrphostin AG1478, AG1024, and MMP2/9 inhibitor were purchased from Calbiochem (La Jolla, CA). The following antibodies were obtained from Santa Cruz Biotechnology (Santa Cruz, CA): monoclonal anti-IGF-IR  $\beta$ -domain antibody (3B7), monoclonal EGFR antibody (R-1), and polyclonal anti-IGF-IR antibody (C-20). The horseradish peroxidase-conjugated monoclonal anti-phosphotyrosine antibody (4G10) and polyclonal anti-EGFR antibody (06-129) were obtained from Upstate Biotechnology (Charlottesville, VA). Polyclonal anti-active MAPK antibody (9101) and anti-MAPK (9320) are from Cell Signaling Technology (Danvers, MA). The polyclonal HB-EGF neutralization antibody was from R&D Systems.

### Cell culture and siRNA transfection

Detailed description of the tissue culture methods and siRNA transfection techniques have been described previously (8). Briefly, MCF-7 cells growing in 5% FBS-IMEM were routinely maintained in a humidified 95% air, 5% CO<sub>2</sub> incubator at 37 C, and 24 h before the treatment, the medium was changed into phenol red-free IMEM supplemented with 1% dextran-coated charcoal-stripped (DCC)-FBS for 24 h. Cells were then treated with different agents as indicated and collected for assays. For transfection experiments with siRNA directed against IGF-IR and the EGFR, the medium for MCF-7 cells was first changed into antibiotic-free and serum-free DMEM without phenol red (Gibco Life Technologies) for 2 h. Cells were then transfected with siRNA that was nonspecific (siControl) or against the selective proteins at 50 pmol/ml. The transfection reagent was DharmaEFCT (Dharmacon), and the procedure was carried out according to the manufacturer's instructions. After 6 h, fresh IMEM containing 5% DCC-FBS was added to bring the volume to 2 ml/well in total. Two days later, cells were extracted for Western blotting.

### Isolation of total RNA and RT-PCR analysis

Total cellular RNA was isolated from the cells using TRIzol reagent (GIBCO BRL, Rockville, MD). The primers and probes for TaqMan assays of IGF-IR and EGFR were synthesized in the Core laboratories at the University of Virginia. The paired primers for IGF-IR are forward 5'-TTGCAAGGAAAGAAATTCAAACAC-3' and reverse 5'-CCTAGGAACAGAGAAAATGTCAACAA-3'. The paired primers for EGFR are forward 5'-GGTTCCTTCTGCCCTCTGT-3' and reverse 5'-

GCAGCCAGTTTGTATTGAGATGT-3'. To account for differences in starting material, quantitative PCR was also carried out for each cDNA sample using the housekeeping genes human glyceraldehyde-3-phosphate dehydrogenase (GAPDH). The primers for GAPDH were synthesized by the Core laboratory of the University of Virginia, and the sequences are 5'-CCACCCATGGCAAATTCCATGGCA-3' and reverse 5'-TCTAGACGGCAGGTCAGGTCCACC-3'. RT was then performed using MultiScribe reverse transcriptase (Applied Biosystems, Foster City, CA) and random hexamers per the manufacturer's instructions. Quantitative PCRs were performed in triplicate for each sample using equal amounts of each cDNA sample equivalent to 50 ng starting total RNA. PCR amplification and monitoring of the fluorescent emission in real time were performed in the ABI Prism 7900HT sequence detection system (Applied Biosystems) as described. The data collected from these quantitative PCRs defined a threshold cycle number (Ct) of detection of the target or the housekeeping genes in each cDNA sample. Results were then plotted showing the mean and upper and lower boundaries of the six replicates.

### Immunoprecipitation and immunoblotting

Immunoprecipitation and immunoblotting were carried out as reported by us previously (21). Briefly, cells were washed once with ice-cold PBS containing 1mM Na<sub>2</sub>VO<sub>4</sub> and extracted with binding buffer [50mM Tris (pH 8.0), 150mM NaCl, 5mM EDTA, 5% glycerol, 1% Triton X-100, 25 mM NaF, 2 mM Na<sub>2</sub>VO<sub>4</sub>, and 10 µg/ml each of aprotinin, leupeptin, and pepstatin]. Cell lysates were centrifuged at 14,000 × g for 10 min at 4 C to pellet insoluble material. The protein concentration of the supernatant was determined using a DC protein assay kit based on the Lowry method (Bio-Rad). Equal amounts of proteins from cell extracts (0.5 mg) of each treatment were immunoprecipitated using one of the following antibodies: 1 µg monoclonal anti-IGF-IR β-domain antibody (3B7; Santa Cruz Biotechnology) or 1.2 µg monoclonal EGFR antibody (R-1; Santa Cruz Biotechnology). Incubations proceeded for 4 h at room temperature or overnight at 4 C in the presence of 35 µl 50% slurry protein G-Sepharose beads (Gibco Life Technologies). The beads were washed three times in cold binding buffer. For Western blotting, the proteins (either eluted from the beads or from the whole-cell extracts) were analyzed on 7.5% SDS-polyacrylamide gels and transferred to polyvinylidene difluoride (PVDF) membranes. The PVDF membranes were probed with one of following primary antibodies: horseradish peroxidase-conjugated monoclonal anti-phosphotyrosine antibody (4G10; Upstate Biotechnology), polyclonal anti-IGF-IR antibody (C-20; Santa Cruz Biotechnology), polyclonal anti-EGFR antibody (06-129; Upstate Biotechnology), polyclonal anti-active MAPK antibody (9101; Cell Signaling), anti-active Akt (9271; Cell Signaling) antibody, polyclonal anti-Akt (9272; Cell Signaling), or MAPK (9320; Cell Signaling) antibody. After washing the PVDF membrane, the immunoblots were incubated with horseradish peroxidase-conjugated secondary antibodies for 1 h (donkey antirabbit IgG was from Pierce, Rockford, IL; or sheep antimouse IgG was from Amersham, Piscataway, NJ) and further developed using the chemiluminescence detection system (Pierce). The phosphorylation status of MAPK from whole-cell extract was assayed using an antibody recognizing phospho-p42/44 MAPK (9101s; Cell Signaling).

### Assessment of cell growth and apoptosis

Both cell growth and apoptosis assays were detailed previously by us (22). Cells growing in six-well plates were treated with the factors as indicated. After growth for the times specified in the figures, cells were rinsed once with 0.9% saline and then lysed in ZAP buffer [0.01 M HEPES (pH 7.2), 1.5 mM MgCl<sub>2</sub> and 0.13 M ZAP (ethylhexadecyldimethylammonium bromide; Kodak, Rochester, NY)]. The released nuclei in 1 ml ZAP buffer were mixed with 9 ml Isoton II diluent (catalog no. 23-375-212; Coulter Corp., Miami, FL) and counted with a model Z1 Coulter counter. Cell apoptosis was assayed by measuring cellular DNA fragmentation with a commercially available kit (the Cell Death Detection ELISA Plus kit; Roche Molecular

Biochemicals, Indianapolis, IN). Cell extracts of each sample were prepared and analyzed according to the manufacturer's protocol and were read on a plate reader at 405 nm. The quantity of cleaved DNA measured by ELISA as an indicator of apoptosis was normalized to the number of cells present.

### Confirmation of mycoplasma-free cell lines

The cells used in this investigation were tested for mycoplasma contamination with a luminometer-based kit, which detects mycoplasma contamination by measuring mycoplasma enzyme activities (Myco-Alert; Carnbrex BioScience, Baltimore, MD). When mycoplasma was detected, the sample was verified using a PCR-based test (Stratagene, La Jolla, CA). All passages of the cells contaminated with mycoplasma were excluded from further evaluation.

### Statistical analysis

All reported values are the means  $\pm$  SEM. Statistical comparisons were determined with one-way ANOVA. Results were considered statistically significant if the *P* value was <0.05.

## Results

### Rapid activation of IGF-IR and EGFR by E2 in MCF-7 breast cancer cells

Our initial approach was to demonstrate the presence of the IGF-IR and EGFR receptors by Western blot in MCF-7 cells and then to quantitate the levels of message by real-time PCR. MDA-MB-231 cells, which have high expression of EGFR, were used as a positive control for EGFR expression. Figure 2A shows a strong IGF-IR immunoprotein band and a much weaker EGFR band from MCF-7 cell extracts on Western blot (*left*). With quantitative RT-PCR, we also demonstrated that the IGF-IR mRNA level was substantially higher than that of EGFR (*right*). To investigate whether E2 rapidly increases the phosphorylation status of IGF-IR and EGFR, MCF-7 cells were treated with vehicle or E2 for 5 min. As shown in Fig. 2B, E2 increased the phosphorylation status of the IGF-IR (*left*) and the EGFR (*right*) when compared with the vehicle-treated controls. As expected, the cognate ligands IGF-I and EGF increased receptor phosphorylation to a greater extent than did E2.

### IGF-IR acts upstream of the EGFR

To demonstrate the role of IGF-IR on EGFR activation, we first used the reductionist strategy with the cognate ligands themselves to interrogate the upstream/downstream nature of the IGF-IR/EGFR relationship. Figure 3A shows that both IGF-I and EGF increased the phosphorylation status of EGFR in a dose-dependent manner. Unlike EGFR, the phosphorylation status of IGF-IR was increased only by its ligand IGF-I but not by EGF (Fig. 3B), providing evidence that IGF-IR is an upstream molecule of EGFR in the IGF-I signaling cascade. To demonstrate whether MMP is required for IGF-I-induced EGFR activation, cells were treated with IGF-I in the presence of a selective IGF-I inhibitor (AG1024), a selective EGFR inhibitor (AG1478), or an inhibitor for MMP2 and MMP9 (MMP2/9 inhibitor). As shown in Fig. 3C (*top and bottom*), both AG1024 and the MMP2/9 inhibitor significantly attenuated IGF-I-induced EGFR activation, supporting that IGF-IR, MMP2, and MMP9 are molecules upstream of EGFR activation in the IGF-I signaling pathway. AG1478 as a positive control markedly inhibited EGFR phosphorylation induced by IGF-I. In contrast with IGF-I-induced EGFR phosphorylation, EGFR phosphorylation induced by its ligand EGF was blocked only by AG1478 but not by AG1024 (supplemental Fig. 1, published as supplemental data on The Endocrine Society's Journals Online web site at <http://endo.endojournals.org>), supporting that the IGF-I is an upstream molecule on EGFR activation.



## E2 acts through the IGF-IR and EGFR

E2 rapidly induces EGFR activation in breast cancer cells (23), but it is unknown whether IGF-IR plays a role as an upstream molecule in E2-induced EGFR phosphorylation. Accordingly, we tested whether E2 co-opts the IGF-IR pathway on EGFR activation in MCF-7 cells. As shown in Fig. 4A, E2 rapidly increased EGFR phosphorylation, which was abrogated by the presence of AG1024 and the MMP2/9 inhibitor. The result indicates that both IGF-IR and MMP2/9 are upstream molecules of EGFR in the E2 rapid signaling pathway. To further confirm our observation, we investigated the E2 effect on EGFR phosphorylation after knocking down the IGF-IR with a selective siRNA. Successful knocking down of IGF-IR with selective siRNA is shown in Fig. 5B, and the method has been reported by us previously (8). As shown in Fig. 4B, treatment with E2 greatly increased EGFR phosphorylation. Knocking down of IGF-IR with expression of siRNA did not alter the basal level of EGFR phosphorylation status when compared with that of the control but significantly attenuated E2-induced EGFR activation (Fig. 4B, *bottom*). Together, our data demonstrated the upstream role of IGF-IR in E2 action on the activation of EGFR in MCF-7 breast cancer cells.

## IGF-IR is an upstream molecule on EGFR-dependent MAPK activation

While demonstrating that E2 induces IGF-IR and EGFR phosphorylation in a linear fashion, we considered it necessary to link this to MAPK activation. We first tested three MCF-7 cell variants from different laboratories to see whether blockade of MMP2, MMP9, and EGFR can affect IGF-I-induced MAPK activation. This again represented the reductionist strategy, allowing us to focus on effects mediated by the IGF-IR. Cell line A was from our own laboratory, line B from Dr. Norman (University of California-Riverside), and line C from ATCC (Manassas, VA). We observed that IGF-I-stimulated MAPK activation was significantly attenuated by both the MMP2/9 inhibitor and AG1478 (Fig. 5A, *top* and *bottom*). These data indicated that MMP2/9 and EGFR acted downstream of IGF-IR with respect to activation of MAPK.

We then employed a dual strategy using both selective kinase inhibitors and siRNAs to investigate the ranking order of IGF-IR and EGFR on MAPK activation. Accordingly, we selectively knocked down IGF-IR or EGFR using siRNAs against IGF-IR or EGFR based on the protocols described by us previously (8). Our initial experiments confirmed the degree of knockdown. The expression of these proteins was detected on Western blot and examined carefully for evidence of specificity of knockdown. When MCF-7 cells were transfected with the siRNA directed against IGF-IR, the levels of this protein were decreased 48–72 h after transfection and reached less than 2–5% when compared with levels of IGF-IR in the cells transfected with nonspecific scrambled siRNA (Fig. 5B, *left*). The siRNA against EGFR exerted similar specific effects (Fig. 5B, *right*). Expression of the selective siRNA against either IGF-IR or EGFR has little effect on protein levels of ER $\alpha$  and Shc from the same cell extract. These experiments demonstrated that siRNAs against IGF-IR or EGFR were specific and effectively down-regulated the selective target proteins in MCF-7 cells.

We then used the dual-strategy tools to decipher the mechanistic roles of IGF-IR and EGFR in their ligand-induced MAPK activation. The *left panel* of Fig. 5C shows that knockdown of IGF-IR did not affect the basal level of MAPK activity. Treatment of the cells with IGF-I and EGF resulted in a 9- and 12-fold increase of MAPK phosphorylation in nonspecific scrambled siRNA transfected cells, respectively. However, knockdown of IGF-IR with the selective siRNA significantly inhibited IGF-I-stimulated, but not EGF-stimulated, MAPK phosphorylation. Our data suggest that IGF-IR does not maintain the basal MAPK activity and has no effect on EGF-induced MAPK activation. The *right panel* of Fig. 5C shows that knockdown of EGFR with siRNA significantly decreased the basal level of MAPK phosphorylation. IGF-I and EGF alone induced MAPK phosphorylation to 7- and 12-fold over

the control, respectively. Expression of siRNA against EGFR totally blocked EGF-induced MAPK activation but only partially attenuated MAPK phosphorylation induced by IGF-I. These results clearly indicate that the IGF-IR signals through the EGFR to activate MAPK and support the concept of a linear pathway. However, some of the effects of IGF-IR-regulated MAPK activation appear to be independent of the EGFR because knockdown of EGFR with selective siRNA did not completely block MAPK activation induced by IGF-I. Our results also indicate that the EGFR plays a role maintaining the basal level of MAPK activation in breast cancer cells.

To confirm the above observations, we again used AG1024, AG1478, and MMP2/9 inhibitor and tested the effect of inhibitors on ligand-induced MAPK activation. As shown quantitatively in Fig. 5D (*left*), IGF-I at 20 ng/ml strongly stimulated MAPK phosphorylation, which was inhibited by AG1024, AG1478, and MMP2/9 inhibitor. These data further suggest that EGFR, MMP2, and MMP9 are all downstream of IGF-IR on IGF-I-stimulated MAPK phosphorylation. Unlike IGF-I, EGF-stimulated MAPK phosphorylation is sensitive only to AG1478 but insensitive to AG1024 and MMP2/9 inhibitor (Fig. 5D, *right*). In the previous section, we demonstrated that IGF-IR is required for E2 to activate EGFR. Now we show that EGFR-dependent MAPK activation is part of the downstream signal of IGF-IR activation. Together, our data support that E2-induced MAPK activation uses a linear cascade of IGF-IR, MMP, and EGFR.

#### IGF-IR, EGFR- and HB-EGF involvement in E2-induced MAPK activation

We next examined the roles of the IGF-IR, EGFR, and HB-EGF in mediating E2 stimulation of MAPK activation with our dual strategy of specific inhibitors and siRNA. As shown in Fig. 6A, E2 greatly increased MAPK phosphorylation in MCF-7 cells. Knockdown of either IGF-IR or EGFR with siRNA inhibited E2-induced MAPK phosphorylation while not altering the basal levels (*right*), suggesting that both IGF-IR and EGFR are involved in E2-induced MAPK activation. Both AG1024 and AG1478, the selective receptor tyrosine kinase inhibitors of IGF-IR and EGFR, also blocked E2-induced MAPK phosphorylation (*left*), further supporting that IGF-IR and EGFR are molecules involved in E2 rapid action in breast cancer cells. To demonstrate the involvement of HB-EGF in E2-induced MAPK activation, an HB-EGF-neutralizing antibody was employed. Figure 6B shows that E2 significantly increased MAPK activation compared with the control. In the presence of HB-EGF antibody, the E2-induced MAPK phosphorylation was significantly blocked. The above results support the fact that E2 activates a cascade event involving IGF-IR, MMP, HB-EGF, and EGFR, leading to the activation of MAPK.

#### Biological effects of E2 in comparison with IGF-I and EGF on cell growth

After demonstration of the molecular involvement of IGF-IR and EGFR on E2-induced MAPK activation, we wished to assess the biological consequences of both receptors on E2 action in MCF-7 cells. As biological endpoints, we counted cell numbers to examine cell growth in response to E2 and to the downstream mediators IGF-I and EGF. For this purpose, the dual knockdown and inhibitor strategies were again employed. Cells were transfected with the selective siRNA against either IGF-IR or EGFR, and then cell numbers were counted on d 4 after treatment with E2, growth factors, or vehicle (ethanol). As shown in Fig. 7A, the cell numbers in nonspecific siRNA transfected groups were  $0.68 \times 10^6$  cells per well in vehicle-treated,  $2.3 \times 10^6$  cells per well in E2-treated,  $1.7 \times 10^6$  cells per well in IGF-I-treated, and  $1.2 \times 10^6$  cells per well in EGF-treated groups. Knockdown of either IGF-IR or EGFR in vehicle-treated cells significantly decreased the basal levels of cell number to  $0.47 \times 10^6$  and  $0.36 \times 10^6$  cells per well, respectively. Compared with vehicle treatment, knockdown of IGF-IR significantly inhibited E2- or IGF-I- but not EGF-induced stimulation of cell number, suggesting that ligand-induced EGFR activation is a downstream event in E2 or IGF-I action.

At the same time, knockdown of EGFR with the siRNA significantly retarded the stimulatory effect induced by E2, IGF-I, and EGF, supporting that EGFR is a common converging point mediating ER $\alpha$  and IGF-IR action. Together, these results reinforce our hypothesis that EGFR is a downstream signal molecule required for E2- and IGF-I-induced cell growth stimulation.

Similar results were found with the use of inhibitors. Compared with vehicle-treated cells ( $0.48 \times 10^6$  cells per well), both AG1024 and AG1478 significantly decreased cell number to  $0.39 \times 10^6$  and  $0.37 \times 10^6$  cells per well, respectively (Fig. 7B). E2, IGF-I, and EGF all significantly stimulated cell growth to  $1.4 \times 10^6$ ,  $0.78 \times 10^6$ , and  $0.69 \times 10^6$  cells per well, respectively. Blockade of IGF-IR with AG1024 inhibited only E2- and IGF-I-induced, but not EGF-induced, cell growth. Treatment of cells with AG1478 significantly blocked all E2, IGF-I, and EGF-induced cell number increments. Above observations suggest that IGF-I and EGFR are both involved in E2 biological action and that EGFR is a downstream molecule of IGF-IR activation. Because a decrease in cell number can result either from reduced growth or increased apoptosis, we further investigated whether blockade of IGF-IR or EGFR could inhibit the effects of E2 on cell death protection. As a marker of apoptosis, we analyzed DNA fragmentation by ELISA. MCF-7 cells were pretreated with either AG1024 or AG1478 for 30 min and then treated with E2, IGF-I, or EGF for 3 d. As shown in Fig. 7C, a statistically significant, approximately 2-fold increase of apoptosis was observed in both AG1024- and AG1478-treated groups when compared with the cells treated with vehicle. Treatment of cells with E2, IGF-I, and EGF significantly decreased cell death rate compared with vehicle-treated control. Both inhibitor AG1024 and AG1478 diminished the E2-, IGF-I-, and EGF-induced antiapoptotic effect. Interestingly, AG1024 had little effect on EGF-induced cell growth (Fig. 7B) but significantly inhibited EGF-induced cell death protection. The result suggests that a nonspecific blockade of cell survival regulated by IGF-IR and PI3K/Akt pathways surpassed the EGF-stimulated cell growth. Together, the data indicate that both IGF-IR and EGFR play a role in the action of E2 to protect against cell death, in which IGF-IR might exert stronger antiapoptotic effect than EGFR.

## Discussion

The present study demonstrated for the first time that E2 co-opts a linear pathway involving the IGF-IR, MMPs, and HB-EGF that leads to activation of EGFR-dependent MAPK in MCF-7 breast cancer cells (Fig. 1). Our hypothesis is supported by the following evidence: 1) E2 rapidly induces IGF-IR, EGFR, and MAPK activation in MCF-7 cells; 2) blockade or knockdown of IGF-IR and MMP not only inhibits E2-induced EGFR phosphorylation but also abrogates E2-induced MAPK phosphorylation; 3) a neutralizing antibody against HB-EGF blocks E2-induced MAPK activation; and 4) knockdown or blockade of IGF-IR inhibits both E2- and IGF-I-induced, but not EGF-induced, cell growth. To further support our hypothesis that the EGFR serves as a nodal point in E2 rapid action in breast cancer cells, a reductionist strategy was used to more precisely examine the upstream/downstream relationships between IGF-IR and EGFR in the absence of E2. This allowed confirmation that the linear pathway of sequential activation of IGF-IR, MMP, and EGFR is required for E2-induced MAPK activation in MCF-7 cells. The data showed that 1) knockdown or blockade of IGF-IR abrogated IGF-I-induced, but not EGF-induced, MAPK activation, and as predicted from the model, knockdown or blockade of EGFR blocked both IGF-I- and EGF-induced MAPK, suggesting that IGF-IR acts upstream of EGFR; 2) knockdown or blockade of EGFR nearly completely blocked EGF-induced MAPK phosphorylation but only partially inhibited IGF-I effects, indicating that IGF-IR activates MAPK in both an EGFR-dependent and -independent manner; and 3) MMP2 and MMP9 are both involved in IGF-IR action on MAPK activation.

Roudabush *et al.* (18) have demonstrated that IGF-IR-initiated MAPK activation requires a linear signaling pathway involving the sequential activation of MMP, HB-EGF, and EGFR in



noncancer COS-7 cells. IGF-IR activation induced by E2 was demonstrated in uterine epithelial cells (24,25), in wild-type ER $\alpha$ -transfected COS-7 cells (19), and in MCF-7 breast cancer cells (8). However, the ability of E2 to trigger a downstream cascade involving the IGF-IR, MMP, HB-EGF, and the EGFR has not been previously reported. In agreement with Roudabush *et al.* (18), here we demonstrated that the sequential activation of the IGF-IR, MMP2, and MMP9; proteolytic release of HB-EGF; and activation of EGFR by HB-EGF occurs not only in noncancer cells but also in ER-positive MCF-7 breast cancer cells in both E2 and IGF-I actions.

Before this study, it was unclear why E2 rapid action involved so many signaling molecules, including both IGF-IR and EGFR. Our current findings are highly consistent with the concept that many ligands/receptors use EGFR as a nodal point for MAPK activation (Fig. 1). Although the E2-induced phosphorylation status of both IGF-IR and EGFR is weaker than that induced by their cognate ligands, the sequential activation of IGF-IR, MMP, EGFR, and MAPK by E2 might contribute to important events in E2-induced genomic and nongenomic actions. In agreement with this, our data show that the linear activation of both IGF-IR and EGFR also exists in regulation of both cell growth and antiapoptotic processes in MCF-7 breast cancer cells.

Our model (Fig. 1) predicted that knockdown or blockade of IGF-IR activation prevented E2- and IGF-I-induced, but not EGF-induced, cell growth and that knockdown or blockade of EGFR activation inhibited MCF-7 cell growth induced by E2, IGF-I, and EGF. The observations clearly demonstrated a linear role of the receptors in ligand-induced cell growth. Furthermore, we observed that the IGF-IR inhibitor AG1024 did not block EGF-induced cell growth but significantly reversed EGF-induced cell death protection, suggesting that IGF-IR signaling to Akt activation may play another important role besides MAPK activation on cell mitogenic function. We plan to investigate the PI3K/AKT pathway in the future.

Recently, Ahmad *et al.* (26) reported that the requirement for EGFR-dependent MAPK activation in IGF-I action occurs only in normal human mammary epithelial cells but not in MCF-7 breast cancer cells. In addition, they suggested that formation of a complex between IGF-IR and EGFR, but not the activation of an IGF-IR-MMP-EGFR axis, is the mechanism of IGF-I-induced EGFR activation in breast cancer cells. In contrast with the above report, we here demonstrated that EGFR-dependent MAPK activation in IGF-I action occurs not only in our MCF-7 cells but also in MCF-7 variant cells from two other sources, in which the MMP2/9 inhibitors and AG1478 inhibited the IGF-I-induced MAPK activation. The reason for this discrepancy likely is the result of different experimental conditions and perhaps to our use of E2-deprived DCC medium to study both E2 and IGF-I functions. The medium containing phenol red has trace amounts of E2 and might affect IGF-I action on MAPK activation because the E2 effect on the IGF-I system has been well documented previously (27). It should be noted that we did observe a complex formation between IGF-IR and EGFR in our MCF-7 cells (data not shown). However, our study eliminated the role of the complex in E2 and IGF-I biological actions based on the following findings: 1) the complexes were not altered by IGF-I or E2 treatment and 2) the complexes were not affected by either MMP2/9 inhibitor or IGF-IR inhibitor AG1024. In fact, our results are in agreement with Kuribayashi *et al.* (28) that IGF-IR was found in a complex with EGFR in Ca9-22 squamous carcinoma cell line, but IGF-I-induced EGFR autophosphorylation is MMP and HB-EGF dependent. Interestingly, IGF-IR interaction with and activation of HER2, but not EGFR, was recently reported exclusively in HER2 antibody trastuzumab-resistant cells but not in parental cells, and IGF-I stimulation results in increased phosphorylation of HER2 in resistant cells (29). The physical interaction among IGF-IR, EGFR, and HER2 in breast cancer cells is currently under investigation in our laboratory.

Our experimental strategy used several selective inhibitors. Two of them are the inhibitors of IGF-IR and EGFR tyrosine kinases, AG1024 and AG1478. These compounds are tyrphostins belonging to a family of synthetic protein tyrosine kinase inhibitors that selectively inhibit receptor autophosphorylation. Because of substitutions on its core structure, the benzylidene malononitrile nucleus, these compounds exert relatively selective inhibition of various tyrosine kinases (30). AG1024 shows a strong tendency for inhibition of IGF-IR tyrosine kinase autophosphorylation and AG1478 for EGFR. The third is a MMP2/9 inhibitor, which is a derivative of *N*-sulfonylamino acid (31). The MMP2/9 inhibitor selectively blocks MMP2 and MMP9 that were reported to be involved in E2- and IGF-I-induced EGFR activation (18,32). Because IGF-IR activates EGFR, but not vice versa, the observations that AG1024 and MMP2/9 inhibitor inhibited IGF-I- and E2-induced EGFR phosphorylation further support our hypothesis of a linear activation of IGF-IR, MMP, and EGFR in E2 and IGF-I action. Interestingly, knockdown or blockade of EGFR causes almost 100% abrogation of EGF-induced MAPK phosphorylation but did not fully inhibit IGF-I-induced MAPK activation, suggesting that IGF-IR activation also has other means to activate MAPK that are not EGFR dependent. Regarding this EGFR-independent MAPK activation in IGF-I action, it has been known that Y950 of IGF-IR is a docking site for the adapter protein Shc (33). At the activating stage, phosphorylated IGF-IR directly recruits Shc to Y950 and activates Shc, leading to MAPK activation. This traditional pathway has been named the Shc/MAPK cascade (34). However, it is not known why IGF-IR, after being activated, still requires EGFR to converge its signal on MAPK activation. In addition, the adapter protein IRS-1 is another direct substrate of IGF-IR and links to the IRS-1/PI3K/Akt pathway activation (33). When IRS-1 is activated, its Y895 is a binding site for Grb2 (35). Thus, IGF-IR-initiated IRS-1 activation should also induce MAPK phosphorylation independently of EGFR. In our study, both Ag1024 and the MMP2/9 inhibitor attenuated the biological action of IGF, but full blockade of IGF-IR effects was not achieved. It is postulated that IGF-I might also activate the insulin receptor to bypass IGF-IR blockade because IGF-I has been known to activate the insulin receptor to a certain extent (36). In addition to MMP2 and MMP9, members of the ADAM (a disintegrin and metalloproteinase with multiple members) family that are involved in processing of growth factors and cytokines and shedding of membrane proteins and are not inhibited by the MMP2 / 9 inhibitor (37) might also be involved in E2 and IGF-I biological actions.

Our laboratory and others previously demonstrated that the knockdown or blockade of classical ER $\alpha$  with siRNA or antiestrogen blocked E2-induced MAPK activation, supporting the ER $\alpha$  as a membrane receptor mediating E2 rapid action in MCF-7 cells (8,21,38). In the meantime, an orphan G protein receptor, GPR30, was also reported as an E2 membrane receptor to mediate E2 rapid action in not only ER-positive but also ER-negative breast cancer cells (39). Using MCF-7 cells, we tested GPR30 involvement in E2-induced MAPK activation. Notably, knockdown of GPR30 had little effect on E2-induced MAPK phosphorylation (supplemental Fig. 2, published as supplemental data on The Endocrine Society's Journals Online web site at <http://endo.endojournals.org>). Our data are in agreement with a recent publication that demonstrated that it is ER $\alpha$ , but not GPR30, that transduces E2 rapid signals to activation of cAMP, MAPK, PI3K, and calcium in MCF-7 cells (40). However, the conflicting reports on the role of GPR30 may be a reflection of different cell types.

In summary, we demonstrated in the present study that the mitogenic effects of E2 in ER-positive breast cancer cells co-opt the IGF-IR signaling pathway, initiating the linear activation of MMP and HB-EGF and then EGFR and MAPK (Fig. 1). This linear pathway has been directly linked to E2-induced cancer cell proliferation. Up-regulation or hyperactivation of membrane growth factor receptors, such as IGF-IR, EGFR, and HER2/neu, has been known to be one of the mechanisms of the development of hormone resistance of breast cancer. Therefore, targeting IGF-IR, EGFR, and HER2/neu in combination with an antiestrogen should not only potentiate the anticancer efficacy but also prevent the development of hormone

resistance. Better understanding of the biology and physiology of this linear signaling pathway of E2 will help in developing such innovative therapies.

## Supplementary Material

Refer to Web version on PubMed Central for supplementary material.

## Abbreviations

DCC, Dextran-coated charcoal-stripped  
 E2, 17 $\beta$ -estradiol  
 EGFR, epidermal growth factor receptor  
 ER $\alpha$ , estrogen receptor $\alpha$   
 FBS, fetal bovine serum  
 HB-EGF, heparin-binding EGF  
 HER2, human EGFR-2  
 IGF-IR, IGF-I receptor  
 IMEM, Improved MEM  
 IRS-1, insulin receptor substrate 1  
 MMP, matrix metalloproteinases  
 PI3K, phosphatidylinositol 3-kinase  
 PVDF, polyvinylidene difluoride  
 siRNA, small inhibitory RNA

## Acknowledgments

We thank Dr. L.M Berstein for critical reading of the manuscript and also thank both Dr. E. Hewlett and Dr. J. Garrison of University of Virginia for their helpful discussions.

This research was supported by U.S. Department of Defense Grant DAMD 17-02-1-0610 (to R.X.-D.S.) and National Institutes of Health Grant CA 65622 (to R.J.S).

## References

1. Ali S, Coombes RC. Estrogen receptor  $\alpha$  in human breast cancer: occurrence and significance. *J Mammary Gland Biol Neoplasia* 2000;5:271–281. [PubMed: 14973389]
2. Yee D, Lee AV. Crosstalk between the insulin-like growth factors and estrogens in breast cancer. *J Mammary Gland Biol Neoplasia* 2000;5:107–115. [PubMed: 10791773]
3. Cheskis BJ. Regulation of cell signalling cascades by steroid hormones. *J Cell Biochem* 2004;93:20–27. [PubMed: 15352158]
4. Alexaki VI, Charalampopoulos I, Kampa M, Vassalou H, Theodoropoulos P, Stathopoulos EN, Hatzoglou A, Gravanis A, Castanas E. Estrogen exerts neuroprotective effects via membrane estrogen receptors and rapid Akt/NOS activation. *FASEB J* 2004;18:1594–1596. [PubMed: 15289442]
5. Nicholson S, Wright C, Sainsbury JR, Halcrow P, Kelly P, Angus B, Farndon JR, Harris AL. Epidermal growth factor receptor (EGFr) as a marker for poor prognosis in node-negative breast cancer patients: neu and tamoxifen failure. *J Steroid Biochem Mol Biol* 1990;37:811–814. [PubMed: 2285594]
6. Baserga R, Peruzzi F, Reiss K. The IGF-1 receptor in cancer biology. *Int J Cancer* 2003;107:873–877. [PubMed: 14601044]
7. Santen RJ, Song RX, Zhang Z, Yue W, Kumar R. Adaptive hypersensitivity to estrogen: mechanism for sequential responses to hormonal therapy in breast cancer. *Clin Cancer Res* 2004;10:337S–345S. [PubMed: 14734489]
8. Song RX, Barnes CJ, Zhang Z, Bao Y, Kumar R, Santen RJ. The role of Shc and insulin-like growth factor 1 receptor in mediating the translocation of estrogen receptor alpha to the plasma membrane. *Proc Natl Acad Sci USA* 2004;101:2076–2081. [PubMed: 14764897]

9. Knowlden JM, Hutcheson IR, Barrow D, Gee JM, Nicholson RI. Insulin-like growth factor-I receptor signaling in tamoxifen-resistant breast cancer: a supporting role to the epidermal growth factor receptor. *Endocrinology* 2005;146:4609–4618. [PubMed: 16037379]
10. Hart S, Fischer OM, Prenzel N, Zwick-Wallasch E, Schneider M, Hennighausen L, Ullrich A. GPCR-induced migration of breast carcinoma cells depends on both EGFR signal transactivation and EGFR-independent pathways. *Biol Chem* 2005;386:845–855. [PubMed: 16164409]
11. Adams TE, McKern NM, Ward CW. Signalling by the type 1 insulin-like growth factor receptor: interplay with the epidermal growth factor receptor. *Growth Factors* 2004;22:89–95. [PubMed: 15253384]
12. Ravichandran KS. Signaling via Shc family adapter proteins. *Oncogene* 2001;20:6322–6330. [PubMed: 11607835]
13. Hackel PO, Zwick E, Prenzel N, Ullrich A. Epidermal growth factor receptors: critical mediators of multiple receptor pathways. *Curr Opin Cell Biol* 1999;11:184–189. [PubMed: 10209149]
14. Luttrell LM, Daaka Y, Lefkowitz RJ. Regulation of tyrosine kinase cascades by G-protein-coupled receptors. *Curr Opin Cell Biol* 1999;11:177–183. [PubMed: 10209148]
15. Zwick E, Hackel PO, Prenzel N, Ullrich A. The EGF receptor as central transducer of heterologous signalling systems. *Trends Pharmacol Sci* 1999;20:408–412. [PubMed: 10577253]
16. Hallak H, Seiler AE, Green JS, Ross BN, Rubin R. Association of heterotrimeric G<sub>i</sub> with the insulin-like growth factor-I receptor. Release of G<sub>βγ</sub> subunits upon receptor activation. *J Biol Chem* 2000;275:2255–2258. [PubMed: 10644671]
17. El Shewy HM, Kelly FL, Barki-Harrington L, Luttrell LM. Ectodomain shedding-dependent transactivation of epidermal growth factor receptors in response to insulin-like growth factor type I. *Mol Endocrinol* 2004;18:2727–2739. [PubMed: 15272055]
18. Roudabush FL, Pierce KL, Maudsley S, Khan KD, Luttrell LM. Transactivation of the EGF receptor mediates IGF-1-stimulated shc phosphorylation and ERK1/2 activation in COS-7 cells. *J Biol Chem* 2000;275:22583–22589. [PubMed: 10807918]
19. Kahlert S, Nuedling S, van Eickels M, Vetter H, Meyer R, Grohe C. Estrogen receptor  $\alpha$  rapidly activates the IGF-I receptor pathway. *J Biol Chem* 2000;275:18447–18453. [PubMed: 10749889]
20. Pietras RJ. Interactions between estrogen and growth factor receptors in human breast cancers and the tumor-associated vasculature. *Breast J* 2003;9:361–373. [PubMed: 12968955]
21. Song RX, McPherson RA, Adam L, Bao Y, Shupnik M, Kumar R, Santen RJ. Linkage of rapid estrogen action to MAPK activation by ER $\alpha$ -Shc association and Shc pathway activation. *Mol Endocrinol* 2002;16:116–127. [PubMed: 11773443]
22. Song RX, Mor G, Naftolin F, McPherson RA, Song J, Zhang Z, Yue W, Wang J, Santen RJ. Effect of long-term estrogen deprivation on apoptotic responses of breast cancer cells to 17 $\beta$ -estradiol. *J Natl Cancer Inst* 2001;93:1714–1723. [PubMed: 11717332]
23. Hutcheson IR, Knowlden JM, Madden TA, Barrow D, Gee JM, Wakeling AE, Nicholson RI. Oestrogen receptor-mediated modulation of the EGFR/MAPK pathway in tamoxifen-resistant MCF-7 cells. *Breast Cancer Res Treat* 2003;81:81–93. [PubMed: 14531500]
24. Richards RG, DiAugustine RP, Petrusz P, Clark GC, Sebastian J. Estradiol stimulates tyrosine phosphorylation of the insulin-like growth factor-1 receptor and insulin receptor substrate-1 in the uterus. *Proc Natl Acad Sci USA* 1996;93:12002–12007. [PubMed: 8876252]
25. Richards RG, Walker MP, Sebastian J, DiAugustine RP. Insulin-like growth factor-1 (IGF-1) receptor-insulin receptor substrate complexes in the uterus. Altered signaling response to estradiol in the IGF-I<sup>m/m</sup> mouse. *J Biol Chem* 1998;273:11962–11969. [PubMed: 9565625]
26. Ahmad T, Farnie G, Bundred NJ, Anderson NG. The mitogenic action of insulin-like growth factor I in normal human mammary epithelial cells requires the epidermal growth factor receptor tyrosine kinase. *J Biol Chem* 2004;279:1713–1719. [PubMed: 14593113]
27. Bartucci M, Morelli C, Mauro L, Ando S, Surmacz E. Differential insulin-like growth factor I receptor signaling and function in estrogen receptor (ER)-positive MCF-7 and ER-negative MDA-MB-231 breast cancer cells. *Cancer Res* 2001;61:6747–6754. [PubMed: 11559546]
28. Kuribayashi A, Kataoka K, Kurabayashi T, Miura M. Evidence that basal activity, but not transactivation, of the epidermal growth factor receptor tyrosine kinase is required for insulin-like

- growth factor I-induced activation of extracellular signal-regulated kinase in oral carcinoma cells. *Endocrinology* 2004;145:4976–4984. [PubMed: 15271882]
29. Nahta R, Yuan LX, Zhang B, Kobayashi R, Esteva FJ. Insulin-like growth factor-I receptor/human epidermal growth factor receptor 2 heterodimerization contributes to trastuzumab resistance of breast cancer cells. *Cancer Res* 2005;65:11118–11128. [PubMed: 16322262]
  30. Parrizas M, Gazit A, Levitzki A, Wertheimer E, LeRoith D. Specific inhibition of insulin-like growth factor-I and insulin receptor tyrosine kinase activity and biological function by tyrphostins. *Endocrinology* 1997;138:1427–1433. [PubMed: 9075698]
  31. Tamura Y, Watanabe F, Nakatani T, Yasui K, Fuji M, Komurasaki T, Tsuzuki H, Maekawa R, Yoshioka T, Kawada K, Sugita K, Ohtani M. Highly selective and orally active inhibitors of type IV collagenase (MMP-9 and MMP-2): *N*-sulfonylamino acid derivatives. *J Med Chem* 1998;41:640–649. [PubMed: 9484512]
  32. Razandi M, Pedram A, Park ST, Levin ER. Proximal events in signaling by plasma membrane estrogen receptors. *J Biol Chem* 2003;278:2701–2712. [PubMed: 12421825]
  33. Adams TE, Epa VC, Garrett TP, Ward CW. Structure and function of the type 1 insulin-like growth factor receptor. *Cell Mol Life Sci* 2000;57:1050–1093. [PubMed: 10961344]
  34. Baserga R. The contradictions of the insulin-like growth factor 1 receptor. *Oncogene* 2000;19:5574–5581. [PubMed: 11114737]
  35. Myers MG Jr, Wang LM, Sun XJ, Zhang Y, Yenush L, Schlessinger J, Pierce JH, White MF. Role of IRS-1-GRB-2 complexes in insulin signaling. *Mol Cell Biol* 1994;14:3577–3587. [PubMed: 8196603]
  36. Yu Y, Hao Y, Feig LA. The R-Ras GTPase mediates cross talk between estrogen and insulin signaling in breast cancer cells. *Mol Cell Biol* 2006;26:6372–6380. [PubMed: 16914723]
  37. Higashiyama S, Nanba D. ADAM-mediated ectodomain shedding of HB-EGF in receptor cross-talk. *Biochim Biophys Acta* 2005;1751:110–117. [PubMed: 16054021]
  38. Razandi M, Pedram A, Greene GL, Levin ER. Cell membrane and nuclear estrogen receptors (ERs) originate from a single transcript: studies of ER $\alpha$  and ER $\beta$  expressed in Chinese hamster ovary cells. *Mol Endocrinol* 1999;13:307–319. [PubMed: 9973260]
  39. Revankar CM, Cimino DF, Sklar LA, Arterburn JB, Prossnitz ER. A transmembrane intracellular estrogen receptor mediates rapid cell signaling. *Science* 2005;307:1625–1630. [PubMed: 15705806]
  40. Pedram A, Razandi M, Levin ER. Nature of functional estrogen receptors at the plasma membrane. *Mol Endocrinol* 2006;20:1996–2009. [PubMed: 16645038]



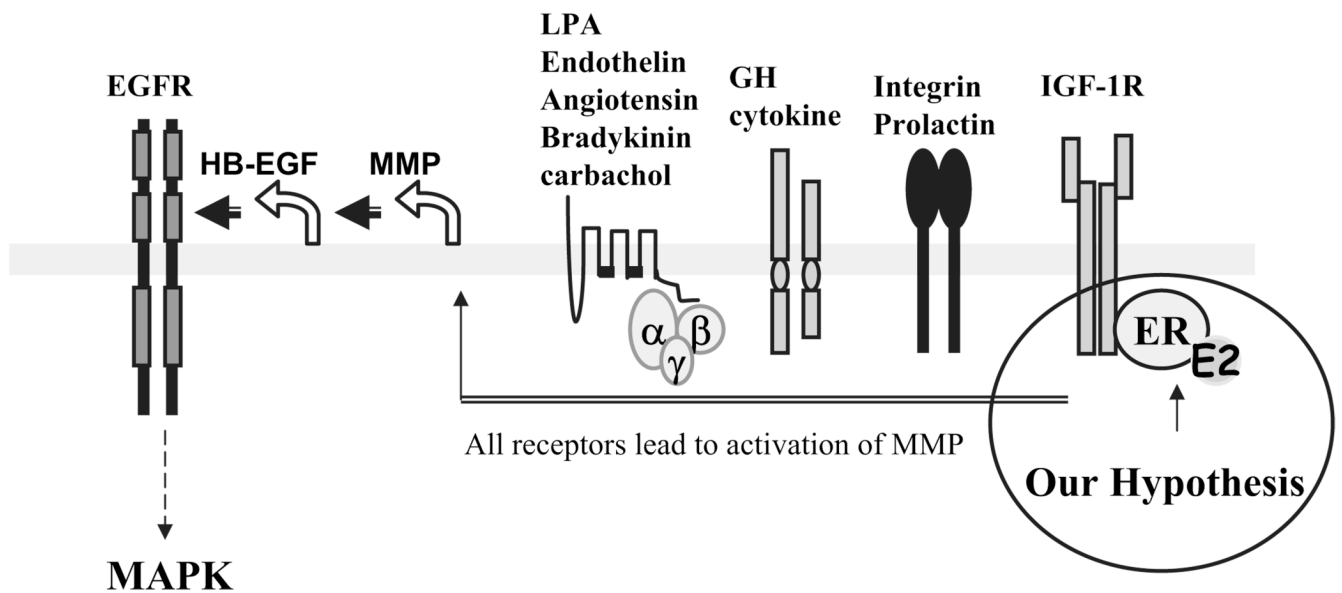


**FIG. 1.**

Model for EGFR-dependent MAPK activation. EGFR acts as a central point linking all upstream ligand signals on MAPK activation. The ligands that lead to the EGFR-dependent MAPK activation can be lysophosphatidic acid (LPA), endothelin, carbachol, angiotensin, bradykinin, GH, prolactin, integrin, and IGF-I. All ligands mediated by their membrane receptors induced MAPK activation via a linear activation of MMP2 and -9, cleavage of HB-EGF, and activation of the EGFR. The *circle on the right* is our proposed pathway of E2-induced MAPK activation. The E2/ER $\alpha$  complex on the cell membrane interacts with IGF-IR and co-opts the IGF-IR pathway to signal through MMP2 and -9, HB-EGF, and the EGFR, leading to the MAPK activation.

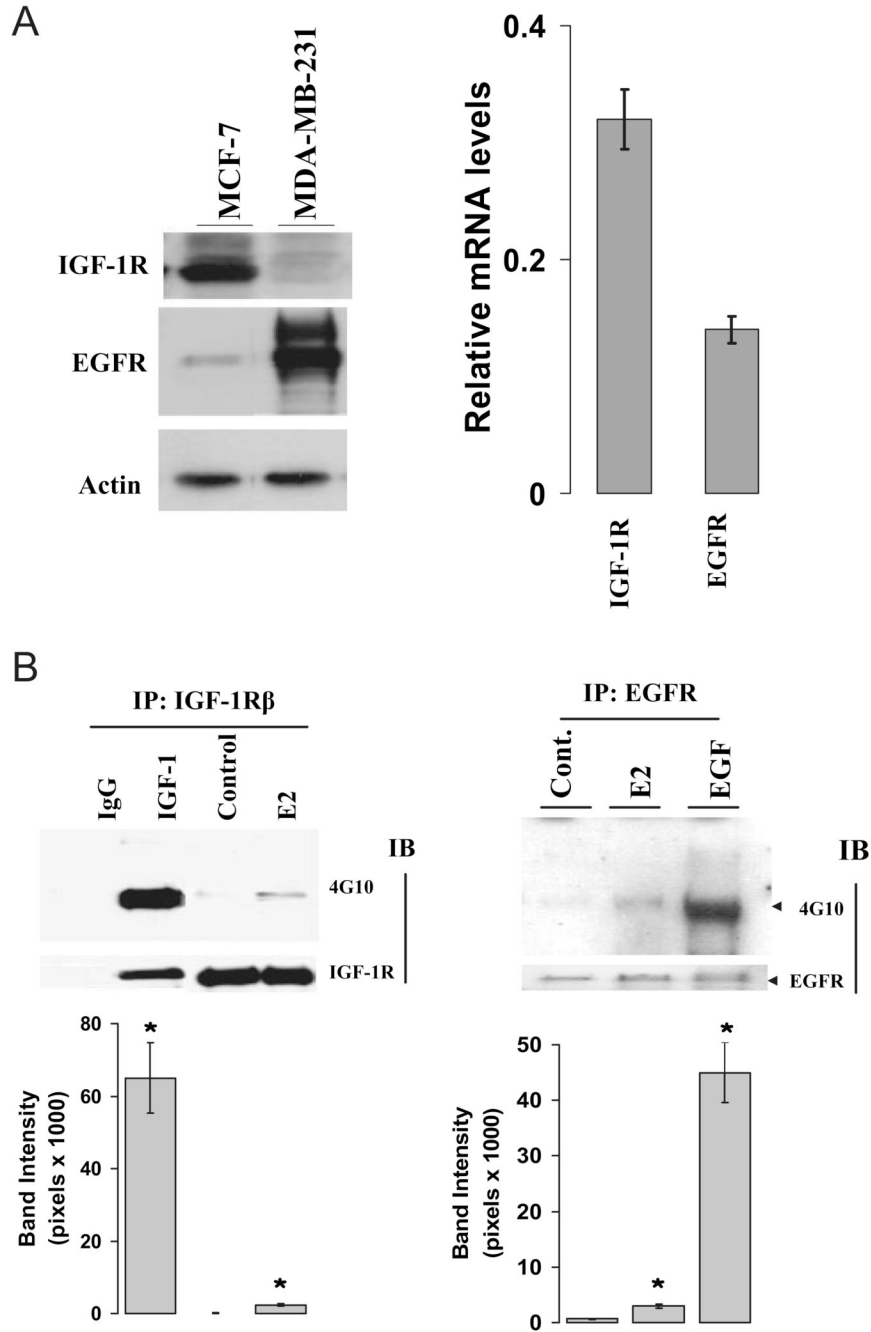


**FIG. 2.** E2 activated both IGF-IR and EGFR in MCF-7 cells. A, Levels of IGF-IR and EGFR expression in MCF-7 cells. Both MCF-7 and MDA-MB-231 cells were extracted from cells at 80% confluence and processed for assessment of IGF-IR and EGFR expression using Western blot (left) and RT-PCR method (right). B, Activation of IGF-IR and EGFR by E2. MCF-7 cells cultured in 1% DCC medium were stimulated with vehicle, 0.1 nM E2, 20 ng/ml IGF-I, or 20 ng/ml EGF for 5 min. Protein lysates were subjected to immunoprecipitation with anti-IGF-IR (left) or anti-EGFR (right) antibodies with subsequent immunoblotting using an anti-phosphotyrosine antibody (4G10) on Western blot. The nonspecific monoclonal IgG antibody was included in the immunoprecipitation step as a negative control. The membranes were

further blotted with either anti- $\beta$ -domain of IGF-IR or anti-EGFR antibodies for total receptor protein loading. All experiments were done at least three times. \*,  $P < 0.05$  compare with the vehicle-treated control.

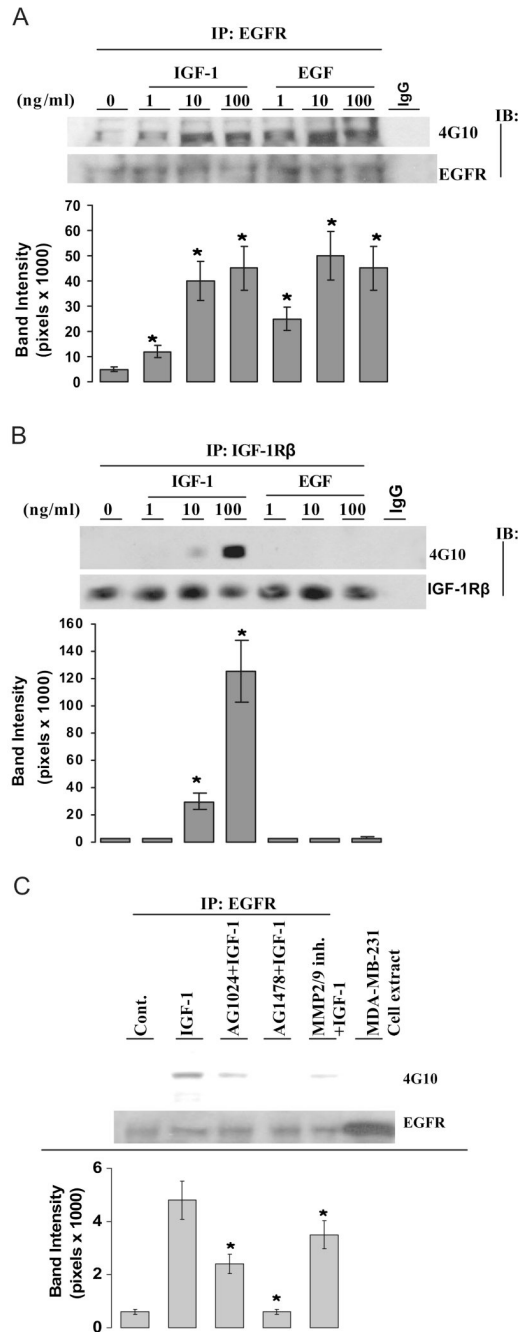


**FIG. 3.** IGF-IR is an upstream molecule of EGFR. A, IGF-I increased the phosphorylation status of the EGFR. Quiescent MCF-7 cells were treated with vehicle, IGF-I, or EGF at doses indicated for 5 min. Lysates were immunoprecipitated with anti-EGFR antibodies. The protein phosphorylation status was detected by 4G10 antibody. The membranes were further blotted with anti-EGFR antibodies for total receptor protein loading. The nonspecific monoclonal IgG antibody was included in immunoprecipitation step as negative control. B, IGF-I, but not EGF, increased the phosphorylation status of the IGF-IR. Cells were challenged with both IGF-I and EGF at doses indicated. The IGF-IR phosphorylation status was assayed as described in Materials and Methods. The membranes were further blotted with anti-IGF-IR antibodies for

total receptor protein loading. The nonspecific monoclonal IgG antibody was included in immunoprecipitation step as negative control. C, Effect of selective inhibitors on IGF-I-induced EGFR activation. Cells were pretreated with 1  $\mu\text{M}$  AG1024, 1  $\mu\text{M}$  AG1478, or 10  $\mu\text{M}$  MMP2/9 inhibitor for 30 min and then treated with vehicle or IGF-I at 20 ng/ml for 5 min. The phosphorylation status of EGFR was assessed as above. The *lower panels* represent the protein loading. The cell lysate from MDA-MB-231 cells was loaded on Western blot to monitor the EGFR molecular weight. Band intensity of EGFR phosphorylation (4G10) in pixels was normalized to the protein loading (EGFR) in the experiment (mean  $\pm$  SEM; n = 3 independent experiments). \*,  $P < 0.05$  compared with the vehicle-treated control (A and B) or compared with IGF-I-treated cells (C).



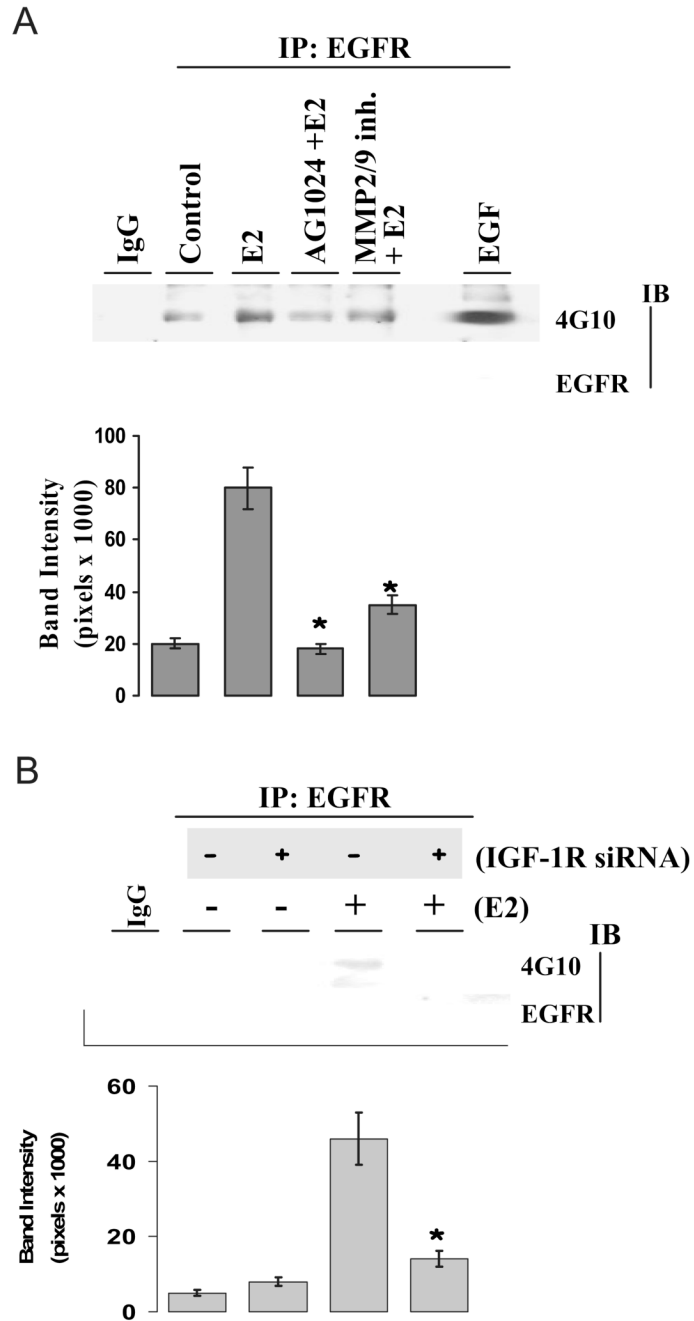


**FIG. 4.** E2-induced EGFR activation involves IGF-IR and MMP. A and B, E2-induced EGFR phosphorylation is dependent on both IGF-IR and MMP. Cells were pretreated with 1  $\mu\text{M}$  AG1024 and 10  $\mu\text{M}$  MMP2/9 inhibitor for 30 min (A) or transiently transfected with nonspecific scrambled siRNA (-) or siRNA against IGF-IR (+) for 3 d (B). Then cells were challenged with vehicle or E2 at 0.1 nM for 5 min. The phosphorylation status of EGFR was assessed as above. Quantitative analysis of the EGFR activation is expressed as band intensity in pixels (*lower panels*), which are further normalized to the protein loading (EGFR) in the same experiment (mean  $\pm$  SEM; n = 5 independent experiments). \*,  $P < 0.05$  compared with E2-treated cells (A) or with E2-treated, scrambled siRNA (-) expression cells (B).

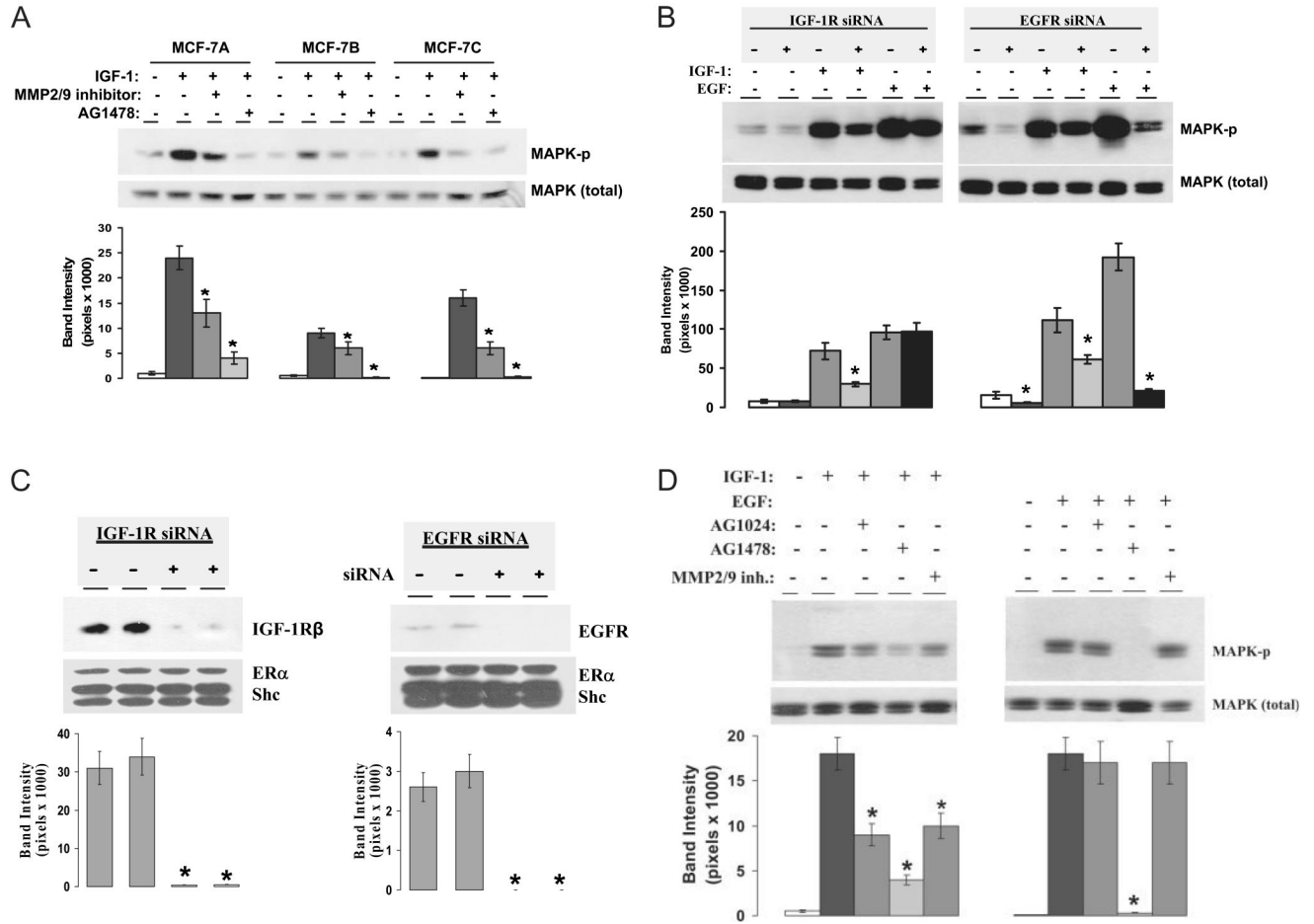


**FIG. 5.** IGF-IR is an upstream molecule on EGFR-dependent MAPK activation. **A**, Effect of AG1478 and MMP2/9 inhibitor on IGF-I-induced MAPK activation in MCF-7 variants. Three variants of MCF-7 cells were pretreated with MMP2/9 inhibitor or AG1478 for 30 min and then treated with vehicle or IGF-I for 15 min. The phosphorylation status and total MAPK protein loading were assayed using specific anti-active and anti-MAPK antibodies. **B**, Knockdown of IGF-IR or EGFR with selective siRNA in MCF-7 cells. Cells were transiently transfected with nonspecific scrambled siRNA (-) or siRNA against IGF-IR and EGFR (+). On d 3, whole-cell extracts in duplicate per treatment were prepared and analyzed by Western blotting as described in Materials and Methods. The PVDF membranes were probed for the expression of IGF-IR (left) or EGFR (right). On each membrane, the protein expression of ER $\alpha$  and Shc was also probed to monitor the specificity of the protein knockdown by siRNA. Quantitative analysis of the protein knockdown is expressed as band intensity in pixels. \*,  $P < 0.05$  compared with the protein levels of control siRNA expression group. **C**, Activation of IGF-IR leads to phosphorylation of both EGFR-dependent and EGFR-independent MAPK. MCF-7 cells were transiently transfected with scrambled siRNA (-) or siRNA against IGF-IR and EGFR(+) for 3 d and then treated with vehicle, IGF-I, or EGF at 20 ng/ml for 15 min. The phosphorylation status and total MAPK were assayed using specific anti-phospho-MAPK or anti-MAPK antibodies (top). **D**, Effect of selective inhibitors on ligand-induced MAPK activation. Cells were pretreated with 1  $\mu$ M AG1024, 1  $\mu$ M AG1478, and 10  $\mu$ M MMP2/9 inhibitor for 30 min and then challenged with vehicle, IGF-I, or EGF at 20 ng/ml for 15 min. The MAPK

phosphorylation status was assayed using cell extracts. Band intensity of MAPK phosphorylation in pixels was normalized to the MAPK protein loading in A, C, and D (mean  $\pm$  SEM; n = 3 independent experiments for each figure). \*,  $P < 0.05$  comparing the inhibitor or siRNA knockdown of IGF-I- or EGF-treated group with the IGF-I- or EGF-treated alone (A, C, and D).

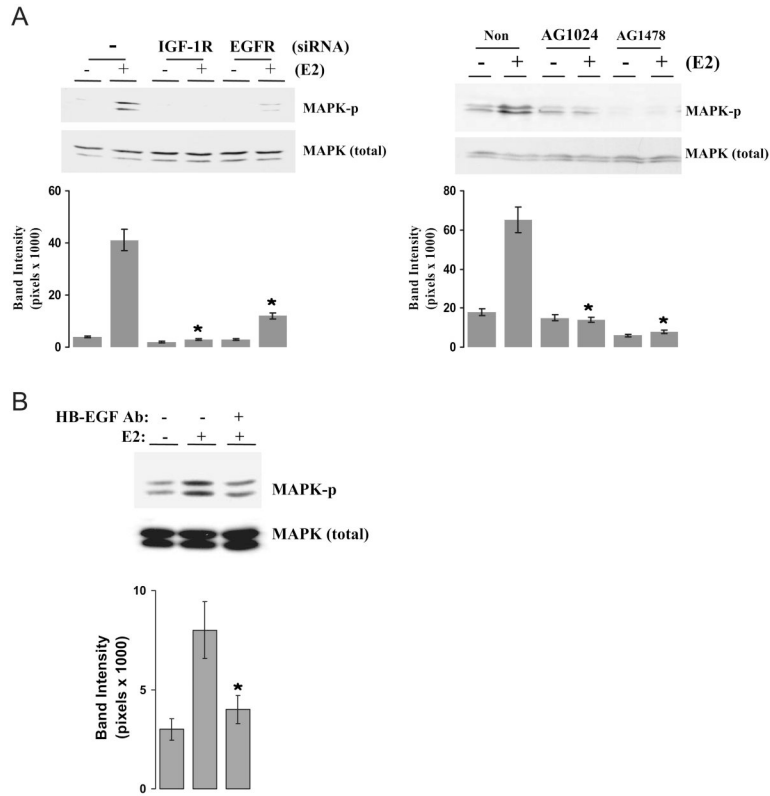


**FIG. 6.** IGF-1R, EGFR, and HB-EGF involvement in E2-induced MAPK activation. **A**, Knockdown or blockade of IGF-1R and EGFR on E2-induced MAPK activation. MCF-7 cells were transiently transfected with nonspecific scrambled siRNA (–) or siRNA against IGF-1R and EGFR (+) (*left*) or pretreated with either 1  $\mu$ M AG1024 or AG1478 for 30 min (*right*). Then cells were challenged with vehicle or 0.1 nM E2 for 15 min. The MAPK phosphorylation was assayed. **B**, HB-EGF is involved in E2-induced MAPK activation. Cells were pretreated with anti-HB-EGF neutralizing antibodies at 10  $\mu$ g/ml and then challenged with vehicle or E2 for 15 min. The MAPK phosphorylation was assayed. Band intensity of MAPK phosphorylation in pixels was normalized to the MAPK protein loading in A and B (mean  $\pm$  SEM; n = 3 independent experiments for each figure). \*,  $P < 0.05$  compared with E2-treated, control siRNA expression cells (A, *left*) or the E2-treated alone (A, *right*, and B).

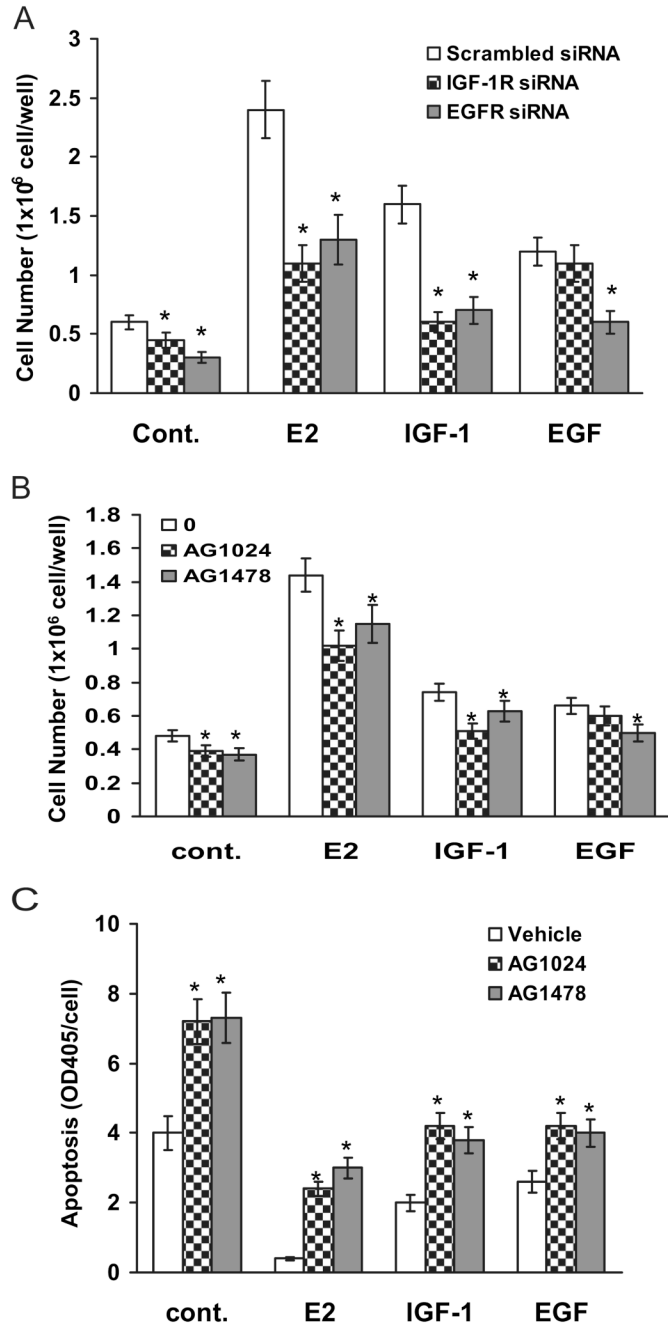


**FIG. 7.** Linear activation of IGF-IR and EGFR is involved in E2-induced cell growth and cell death protection. A and B, Knockdown or blockade of IGF-IR and EGFR on ligand-induced cell growth. Cells were transiently transfected with nonspecific scrambled siRNA or siRNA against IGF-IR and EGFR (A) or pretreated with either 1  $\mu$ M AG1024 or 1  $\mu$ M AG1478 for 30 min (B). Then the cells were challenged with vehicle, E2 at 0.1 nM, 20 ng/ml IGF-I, or 20 ng/ml EGF for 4 d. Cell numbers were counted at the end of experiments. C, Effect of selective inhibitors on E2-induced cell death protection. MCF-7 cells were pretreated with either 1  $\mu$ M AG1024 or 1  $\mu$ M AG1478 for 30 min and then treated with vehicle, 0.1 nM E2, 20 ng/ml IGF-I, or 20 ng/ml EGF. Cell apoptosis was assayed on d 4 as described in Materials and Methods. Data are



mean  $\pm$  SEM (n = 6). \*,  $P < 0.05$  comparing the siRNA-transfected or inhibitor-treated cells with the growth factor-treated alone.